PERGAMON

Journal of Quantitative Spectroscopy & Radiative Transfer 82 (2003) 505–516

Journal of Quantitative Spectroscopy & Radiative Transfer

www.elsevier.com/locate/jqsrt

# Theoretical calculation of the translation-rotation collision-induced absorption in $N_2$–$N_2$, $O_2$–$O_2$, and $N_2$–$O_2$ pairs

J. Boissoles[a], C. Boulet[b], R.H. Tipping[c,*], Alex Brown[c], Q. Ma[d,e]

[a] *Unite Mixté de Recherche P.A.L.M.S. (Physique des Atomes, Lasers, Molécules, et Surfaces), Université de Rennes I, Campus de Beaulieu, 35042 Rennes Cedex, France*

[b] *Laboratoire de Photophysique Moléculaire, CNRS, Université de Paris-Sud, Centre d'Orsay, Bât 350, 91405 Orsay Cedex, France*

[c] *Department of Physics and Astronomy, College of Arts and Sciences, University of Alabama, 206 Gallalee Box 870324 Tuscaloosa, AL 35487-0324, USA*

[d] *Department of Applied Physics, Columbia University, USA*

[e] *Institute for Space Studies, Goddard Space Flight Center, 2880 Broadway, New York, NY 10025, USA*

Received 18 October 2002; received in revised form 17 December 2002; accepted 22 December 2002

**Abstract**

The translation-rotation collision-induced spectra of $N_2$–$N_2$, $O_2$–$O_2$ and $N_2$–$O_2$ mixtures are calculated theoretically. For $N_2$–$N_2$, using the matrix elements for the quadrupole and hexadecapole moments and the isotropic and anisotropic polarizabilities obtained previously from a global analysis of the fundamental band spectra, we obtain numerical values for the zeroth moment that are smaller than the measured values by 9–14%, depending on the temperature. By increasing the value for the matrix element of the isotropic polarizability slightly, good agreement with experiment is obtained. For $O_2$–$O_2$, the theoretical spectrum is significantly smaller than the experimental result. By increasing the matrix element of the hexadecapole moment by a factor of 1.7, we can obtain good agreement. This larger value for the hexadecapole moment will not appreciably affect the agreement found previously in the fundamental region because the hexadecapole contribution to the intensity is very small, unlike the translation-rotation band where it is larger than the contribution due to the quadrupole moment. Using these parameters, we then calculate the collision-induced absorption for $N_2$–$O_2$ mixtures for which no experimental data exist. Finally, we calculate the collision-induced absorption for air, and compare our results with previous work; we express the results for the ratio of the absorption coefficient of air to that of $N_2$–$N_2$ as a function of wavenumber and temperature, $R(\omega, T)$, which can easily be implemented in atmospheric models.



*Keywords:* Collision-induced absorption; Translation-rotation band; Atmospheric molecular pairs

* Corresponding author. Tel.: +1-205-348-5050; fax: +1-205-348-5051.
*E-mail address:* rtipping@bama.ua.edu (R.H. Tipping).

0022-4073/03/$ - see front matter © 2003 Elsevier Ltd. All rights reserved.
doi:10.1016/S0022-4073(03)00174-2

## 1. Introduction

In the Earth's atmosphere, both in the far infrared and infrared regions, there are two main sources for the continuous absorption of radiation over a range of frequencies: the self and foreign water continua [1,2] arising from the far wings of the allowed pure rotational and vibration-rotational dipole transitions, scaling with number density $\rho$ as $\rho^2_{H_2O}$ and $\rho_{H_2O}\,\rho_{N_2}$, respectively, and the collision induced absorption (CIA) scaling as $\rho^2$ for a pure gas or as the product of the $\rho$'s for a binary mixture [3]. In most cases for zenith measurements, the former continua dominate and are included in most atmospheric radiative transfer programs [4]. However, for low humidity conditions such as long-path limb measurements through the stratosphere, the collision-induced fundamental absorptions of $O_2$ and $N_2$ can be important and are also included [5].

In a series of papers [6–9], we have presented new experimental data and theoretical analyses of the collision-induced fundamental absorption spectra of $N_2$–$N_2$, $O_2$–$O_2$, and $N_2$–$O_2$ pairs. We have shown that it is possible to synthesize these spectra accurately using only the quadrupolar and hexadecapolar induction mechanisms containing matrix elements of the multipolar moments and the isotropic and anisotropic polarizabilities obtained from either independent measurements or from ab initio calculations. Most of the intensity in the fundamental band arises from the long-range quadrupolar induction, but to fit the data over a range of temperatures, we had to include a short-range component as well. We found that to reproduce the small "ripple" structure superimposed on top of the broad background [9], it was necessary to consider contributions from metastable dimers. These feature are more apparent at lower temperatures [10,11], but persist even at $T = 300$ K [12].

In the present paper, we extend this analysis to the translation-rotation spectral region (0–400 $cm^{-1}$). A number of published experimental results [13,14] and previous theoretical studies [15,16] are available for $N_2$–$N_2$ for a range of $T$, whereas for $O_2$–$O_2$ there exists only one experimental result at $T = 300$ K [17]. To the best of our knowledge, no experimental data are available for $O_2$–$N_2$ mixtures. Because the fundamental matrix element of the quadrupole moments and the isotropic polarizability of $N_2$ and $O_2$ are comparable, the corresponding spectra of $N_2$–$N_2$, $O_2$–$O_2$, $N_2$–$O_2$ and $O_2$–$N_2$ (where the first molecule makes the vibrational transition), are similar in shape and magnitude. This is not true for the translation-rotation case because the magnitude of the quadrupole matrix element of $O_2$ is smaller by approximately a factor of 4 than that of $N_2$ and, in fact, the largest contribution from $O_2$ arises from the hexadecapolar induction. Thus, compared to $N_2$–$N_2$, the magnitude of the absorption of $O_2$–$O_2$ is very much smaller and the spectrum is broader because of the different selection rules ($\Delta J = \pm 4,\ \pm 2$ and 0) for the hexadecapolar induction.

Because of the availability of more extensive experimental results for $N_2$–$N_2$, some radiation transfer codes include only this contribution; the neglect of the contribution from $O_2$–$O_2$ collision pairs in the atmosphere is not very important, both because of the smaller magnitude as discussed above, and the fact that the number density of $O_2$ is smaller than that of $N_2$ by a factor of 4. However, the absorption by $N_2$–$O_2$ pairs is not negligible and should be included. In a recent paper, Pardo et al. [18] have estimated that in air, the $N_2$–$N_2$ absorption should be increased by a factor 1.29, independent of frequency and temperature; this resulted in better fits to atmospheric transmission measurements made from Mauna Kea during the extremely dry El Niño conditions.

The present paper is organized in the following way. In Section 2, we give a brief discussion of the theoretical expressions used to model the collision-induced absorption; more extensive details

can be found in Refs. [6–9]. In Section 3.1, we first calculate the zeroth moment [3,15] for $N_2$–$N_2$ using the molecular parameters obtained from a global fit of the fundamental band data [8]. While the overall agreement is reasonable, the theoretical absorption profiles are smaller than the measured ones for all $T$. We then adjust the value of the isotropic polarizability matrix element slightly to improve the agreement. In Section 3.2, we repeat the calculations for $O_2$–$O_2$. The agreement with the single experimental result is less good in this case. We increase the hexadecapole moment matrix element to get the best agreement, and obtain a value close to that obtained by Steele and Birnbaum [19]. We note that neither of these adjustments will significantly affect the results previously obtained for the fundamental band. Using the parameters that give the best fits for $N_2$–$N_2$ and $O_2$–$O_2$ enables us to generate theoretically the collision-induced spectra for $N_2$–$O_2$ pairs, and sample results are presented in Section 3.2. In Section 4, we consider the absorption that one would expect for air, assuming that $N_2$ and $O_2$ are uniformly mixed. We calculate the correction factor $R(\omega, T)$ introduced by Pardo et al. [18] as a function of frequency and temperature. This factor, along with accurate results for $N_2$–$N_2$, enable one to model accurately the CIA for air in the far-IR region. The results and conclusions of the present work are discussed in Section 5.

## 2. Theory

In Refs. [6–9], we have given the details of how one can calculate the CIA of pure or binary mixtures of diatomic gases, following the work of Poll and Hunt [20]. We write the absorption coefficient $\alpha(\omega)$ as a function of wavenumber $\omega(\mathrm{cm}^{-1})$ as

$$\alpha(\omega) = \omega(1 - \mathrm{e}^{-\beta\hbar\omega})A(\omega), \tag{1}$$

where $\beta = 1/kT$. We note that in the far-IR, the stimulated emission factor must be included, whereas in the fundamental region, it has been neglected. By considering only binary collisions valid for atmospheric conditions, the function $A(\omega)$ can be written as

$$A(\omega) = \rho^2 G(\omega)/2 \tag{2a}$$

for pure gases or

$$A(\omega) = \rho_1 \rho_2 G(\omega) \tag{2b}$$

for a binary mixture. The function $G(\omega)$ consists of a linear superposition of individual components, $G_n(\omega)$, where in the present case, because all the vibrational quantum numbers are zero, $n$ is specified by the set of integers

$$n \equiv \{J_1, J_1', J_2, J_2', \lambda_1, \lambda_2, \Lambda, L\}, \tag{3}$$

where $J_i$ and $J_i'$ are the initial and final rotational quantum numbers, and the other four integers characterize the induced dipole moment mechanism [6–9]. Explicitly, we include the long-range isotropic quadrupolar induction described by the coefficients (2,0,2,3) and (0,2,2,3); the anisotropic quadrupolar mechanism (2,2,2,3), (2,2,3,3), and (2,2,4,3); the isotropic hexadecapolar mechanism (4,0,4,5) and (0,4,4,5); and the anisotropic hexadecapolar mechanism (4,2,4,5), (4,2,5,5), (4,2,6,5), (2,4,4,5), (2,4,5,5), and (2,4,6,5).

Because of other theoretical approximations, such as ignoring the anisotropic interaction potential and using a Lennard–Jones model for the isotropic potential [6–9], we do not include the short-range dipole moment components because this would involve additional, unknown parameters.

The zeroth moment of the spectrum, $\Gamma_0$, in units of $cm^{-1}$ $amagat^{-2}$ for a pure gas is defined by [15]

$$\Gamma_0 \equiv \frac{1}{\rho^2}\int_{-\infty}^{\infty}\frac{\alpha(\omega)}{\omega(1-e^{-\beta\hbar\omega})}\,d\omega = \sum_n \Gamma_0(n). \tag{4}$$

Explicit expressions for the individual contributions to the moment have been presented previously [6–9] and are not repeated here. We note that this theoretical definition of the zeroth moment is equivalent to the experimental moment of Stone et al. [13]

$$\Gamma_0 = \int_0^{\infty}\frac{\alpha(\omega)\coth(\beta\hbar\omega/2)}{\omega}\,d\omega \tag{5}$$

by using the principle of detailed balance [21]. For later comparisons with the work of Bosomworth and Gush [17] on $O_2$, we define the integrated intensity $S$ in units of $cm^{-2}$ in the usual way

$$S = \int_0^{\infty}\alpha(\omega)\,d\omega. \tag{6}$$

Unlike the zeroth moment, the integrated intensity does not have an explicit theoretical expression although it is useful in practice.

## 3. Spectra

### 3.1. $N_2$–$N_2$ spectra

As the first step in our analysis of the translation-rotation band of $N_2$–$N_2$, we use the molecular parameters obtained previously [8] from the global fit to the fundamental spectra of $N_2$–$N_2$, $O_2$–$O_2$, $N_2$–$O_2$, and $O_2$–$N_2$ to calculate the zeroth moment. The results are presented in Table 1, along with experimental values from Stone et al. [13] for comparison. The theoretical values are consistently lower than the experimental results by approximately 9–14% over the range of $T$ from 228 to

Table 1
Comparison between the experimental measurements [13] and the theoretical calculations using the molecular parameters obtained previously from a global fit of the fundamental band data [8] for the zeroth moment for $N_2$–$N_2$, $\Gamma_0$, in units $10^{-6}$ $cm^{-1}$ $amagat^{-2}$

| $T$ (K) | Experimental result | Theoretical calculations | (obs − calc)/obs (%) |
|---|---|---|---|
| 343 | 35.7 | 31.2 | 12.6 |
| 322.6 | 34.5 | 31.2 | 9.5 |
| 297.5 | 34.4 | 31.3 | 9.0 |
| 272.5 | 35.1 | 31.4 | 10.5 |
| 253.5 | 35.4 | 31.6 | 11 |
| 228.3 | 37.3 | 32.0 | 14 |

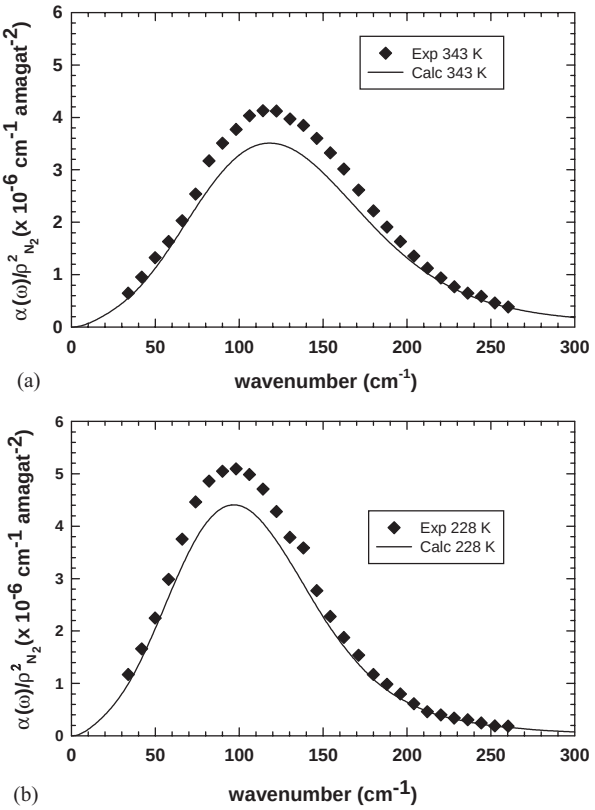


Fig. 1. (a) Comparison between theory and experiment [13] of $\alpha(\omega)/\rho^2$ in units $10^{-6}$ cm$^{-1}$ amagat$^{-2}$ versus wavenumber in cm$^{-1}$ for $N_2$–$N_2$ at $T = 343$ K. The theoretical values were calculated using the parameters determined previously by a global fit to data in the fundamental region [8]. (b) Same as (a) for $T = 228$ K.

343 K. As in our previous work, by knowing the strengths and positions of all the components, we can generate the spectrum by multiplying each component by a normalized line shape and summing. The results obtained using the line shape of Borysow and Frommhold [22] are shown in Fig. 1 for two temperatures. Because in this case the isotropic quadrupolar induction mechanism is dominant, we can easily improve the agreement by increasing slightly the quadrupole moment matrix element, $Q_{00}$, or isotropic polarizability matrix element, $\alpha_{00}$, or both. We choose to increase $\alpha_{00}$ for two reasons: first, in our previous fit to the $N_2$–$N_2$ fundamental spectrum [6], we used the value $\alpha_{00} = 11.74a_0^3$ from accurate radio-frequency refractivity measurements [23] and from $T$-dependent dielectric constant measurements [24]; second, a value $\alpha_{00} = 11.88a_0^3$ was used by Borysow and Frommhold [22] in their work. Both of these are significantly higher than the value $\alpha_{00} = 11.50a_0^3$ we obtained from the global fit [8]. While it would be of interest to perform a global analysis of both the translation-rotation and fundamental band data simultaneously, this is not feasible at the present time, given that data exist for $O_2$–$O_2$ only at one temperature, and the absence of any data for the mixtures in the translation-rotation band. In Fig. 2, we show the improvement obtained with the previously obtained theoretical results [22] at $T = 179$ K, using the larger value $\alpha_{00} = 11.88a_0^3$.

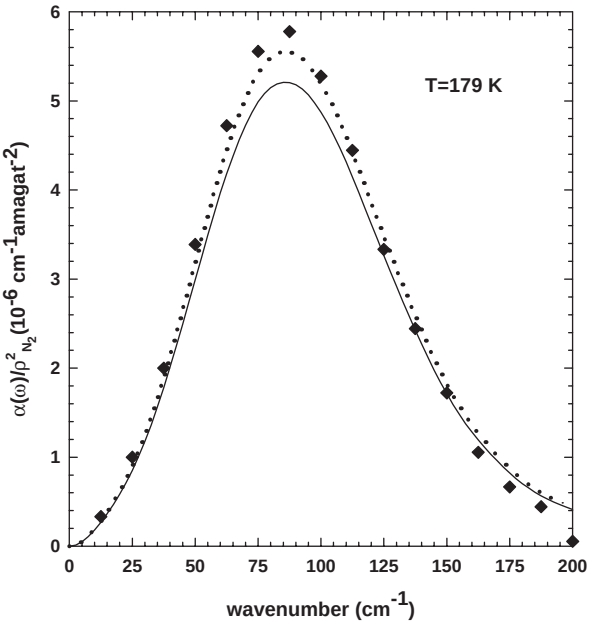


Fig. 2. Comparison between theoretical values of $\alpha(\omega)/\rho^2$ in units $10^{-6}$ cm$^{-1}$ amagat$^{-2}$ versus wavenumber in cm$^{-1}$ for $N_2$–$N_2$ at $T = 179$ K. The solid line is the theoretical spectrum calculated using the previous value for the matrix element of the isotropic polarizability $\alpha_{00} = 11.50a_0^3$; the dashed curve is the result using the value $\alpha_{00} = 11.88a_0^3$; and the ♦ are the theoretical results from Ref. [22].

Similar improvements result for other temperatures as well. Given the experimental uncertainties as well as other simplifications in the theory, we conclude that with the larger value of $\alpha_{00}$ we can accurately model the translation-rotational spectra of $N_2$–$N_2$.

### 3.2. $O_2$–$O_2$ *spectrum*

The only experimental data available for the translation-rotational spectrum of $O_2$–$O_2$ are the data of Bosomworth and Gush [17] taken at $T = 300$ K. Using the values obtained from a global fit of the fundamental band [8], we have synthesized the spectrum and present the results in Fig. 3. We show separately the contributions from the isotropic quadrupole and hexadecapole mechanisms, together with their sum and the experimental results. As in the fundamental band, the anisotropic contributions are small. It can be seen from the figure that, unlike the case of the fundamental, the hexadecapole contribution is approximately 50% of that from the quadrupole mechanism, but the total is considerably smaller than the experimental results. As previously done by Poll and Hunt [15] and Steele and Birnbaum [19], we can increase the value of the previous hexadecapole moment ($\phi_{00} = 4.8ea_0^4$) by a factor of 1.7 ($\phi_{00} = 7.48ea_0^4$) without affecting the corresponding agreement with the fundamental band significantly, because the isotropic quadrupolar mechanism, $Q_{01}\alpha_{00}$, accounts for approximately 90% of the absorption. We note that this value is comparable to that for $N_2$ and close to the value obtained by Steele and Birnbaum [19]. Specifically, these authors obtained for the ratio $(\phi/Q\sigma^2)^2$, where $\sigma$ is the Lennard–Jones parameter, the value of 0.51, whereas we obtain

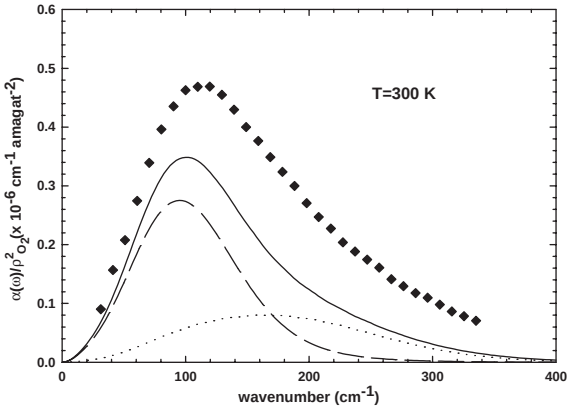


Fig. 3. Comparison between theory and experiment [17] of $\alpha(\omega)/\rho^2$ in units $10^{-6}$ cm$^{-1}$ amagat$^{-2}$ versus wavenumber in cm$^{-1}$ for $O_2$–$O_2$ at $T=300$ K. The total theoretical result calculated within the isotropic polarizability approximation is given by the solid curve, which is the sum of the quadrupolar and hexadecapolar mechanisms calculated using the matrix element $\varphi_{00}=4.4ea_0^4$ found previously, given by the dashed and dotted curves, respectively; the experimental values are denoted by the symbol ♦.

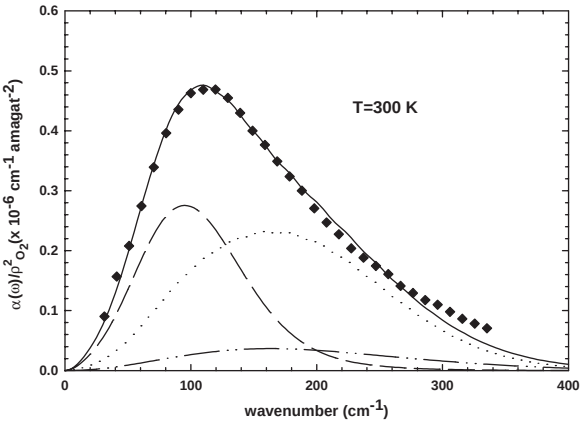


Fig. 4. The same as Fig. 3, except that the hexadecapole matrix element $\varphi_{00}=7.48ea_0^4$ is used and the small anisotropic contributions indicated by the dash double dotted line is included in the total.

the value of 0.47. The improved results are shown in Fig. 4, and the theoretical integrated intensity, $S=8.25\times10^{-5}$ cm$^{-2}$ amagat$^{-2}$, is lower than the experimental value, $S=8.64\times10^{-5}$ cm$^{-2}$ amagat$^{-2}$, by only 4.5%. The theoretical curve falls below the experimental data around 300 cm$^{-1}$, which suggests that a short-range dipole moment may be needed to improve the agreement. However, because the magnitude of the absorption is small and the experimental uncertainties are large in this spectral region, we do not think that it is worthwhile to introduce an extra parameter to improve the fit. Finally, we note that with this increased value for the hexadecapole moment matrix element, this mechanism contributes 150% of that due to the quadrupole mechanism and, as a result, gives rise to a much broader spectrum as can be seen clearly by a comparison between Figs. 1 and 4.

### 3.3. $O_2+N_2$ *mixtures*

Because of the lack of experimental data, the collision-induced spectra for mixtures must be generated by theory, using the parameters obtained as discussed above by fitting the $N_2$–$N_2$ and $O_2$–$O_2$ spectra separately. However, these spectra are precisely what are needed to model the collision-induced absorption in air. In general, if one includes the anisotropic contributions, one cannot separate the system into an "active" molecule (one making a rotational transition) and an "inactive" molecule (one not making a rotational transition). This separation was possible in the fundamental region because the vibrational bands of $N_2$ and $O_2$ occur at different, non-overlapping frequencies. However, because the anisotropic contributions are small (approximately 15%), it is still

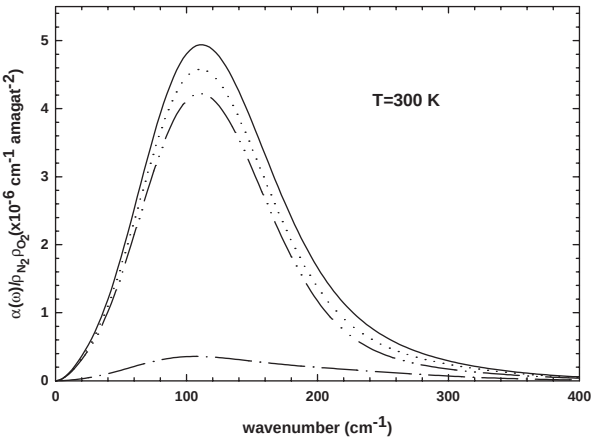


Fig. 5. Theoretical calculation of $\alpha(\omega)/\rho^2$ in units $10^{-6}$ cm$^{-1}$ amagat$^{-2}$ versus wavenumber in cm$^{-1}$ for $N_2$–$O_2$ mixture at $T = 300$ K. Within the isotropic polarizability approximation, the contributions for $O_2$ active and $N_2$ active are given by the dash dotted and dash double dotted lines, respectively. The sum of these two contributions is given by the dotted line, while the exact theoretical value including the anisotropic contributions is given by the solid line.

possible to treat the contributions from $\alpha(O_2)Q(N_2)$ plus $\alpha(O_2)\phi(N_2)$, for which $N_2$ is active, and $\alpha(N_2)Q(O_2)$ plus $\alpha(N_2)\phi(O_2)$, for which $O_2$ is active separately.

The results are presented in Fig. 5, together with their sum and the exact calculations including the anisotropic contributions. As can be seen from the figure, the $O_2$ active contribution is very much smaller than that of the $N_2$ active contribution, as expected from the much smaller magnitude of the quadrupole moment matrix element of $O_2$.

By comparing the sum of the two active contributions with the exact result, one can see that the approximation for the absorption coefficient used by Pardo et al. [18],

$$\alpha(O_2 + N_2)_{\text{exact}} \approx \alpha(N_2 \text{ active–}O_2) + \alpha(O_2 \text{ active–}N_2), \tag{7}$$

that will be discussed at length in the next section, is not too bad.

## 4. Collision-induced absorption in air

For air we write the absorption coefficient, $\alpha_{\text{air}}(\omega)$, as the sum of three terms

$$\alpha_{\text{air}}(\omega) = \alpha(N_2\text{–}N_2)\rho_{N_2}^2 + \alpha(O_2\text{–}O_2)\rho_{O_2}^2 + \alpha(N_2\text{–}O_2)\rho_{N_2}\rho_{O_2}. \tag{8}$$

We assume $\rho(N_2) = 0.79\ \rho_t$, and $\rho(O_2) = 0.21\ \rho_t$, where $\rho_t$ is the total number density of air. Factoring out the absorption of $N_2$–$N_2$, this can be rewritten as

$$\begin{aligned}\alpha_{\text{air}}(\omega) &= 0.624\alpha(N_2\text{–}N_2)\rho_t^2\left[1 + \frac{0.044\alpha(O_2\text{–}O_2)}{0.624\alpha(N_2\text{–}N_2)} + \frac{0.166\alpha(N_2\text{–}O_2)}{0.624\alpha(N_2\text{–}N_2)}\right] \\ &= \alpha_{N_2\text{–}N_2}(\omega)[1 + \varepsilon(\omega, T)] \equiv \alpha_{N_2\text{–}N_2}(\omega)R(\omega, T).\end{aligned} \tag{9}$$

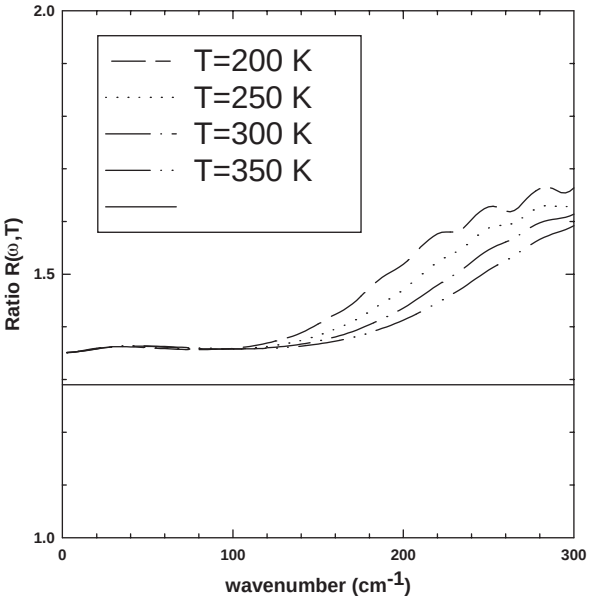


Fig. 6. The correction factor $R(\omega, T)$ as a function of wavenumber in $\mathrm{cm}^{-1}$ for $T = 200, 250, 300$, and 350 K, are given by the dashed, dotted, dash dotted and dash double dotted curves, respectively. The constant value 1.29 inferred by Pardo et al. [18] is shown for comparison by the solid line.

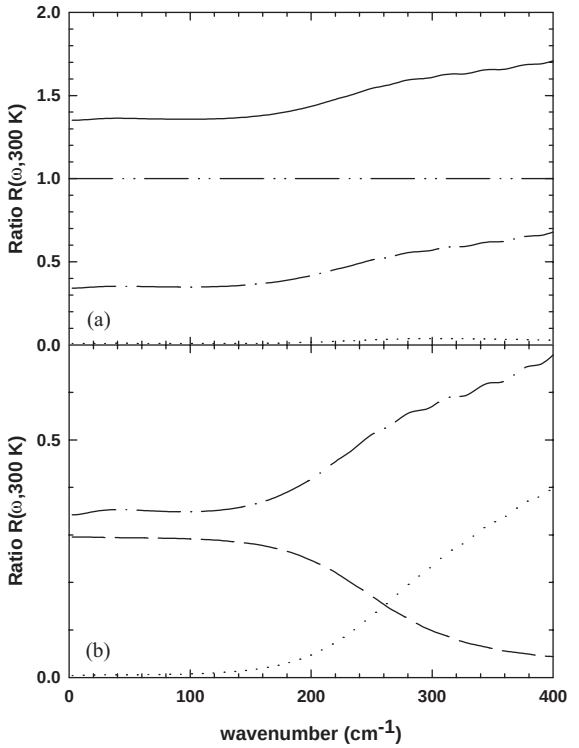


Fig. 7. (a) The contributions to the correction factor $R(\omega, 300\ \mathrm{K})$ as a function of wavenumber in $\mathrm{cm}^{-1}$. The contributions from $O_2$–$O_2$, $N_2$–$O_2$, and $N_2$–$N_2$ are given by the dotted, dash dotted, and dash double dotted curves, respectively; the sum of these, $\alpha_{\mathrm{air}}(\omega)/\alpha_{\mathrm{N_2-N_2}}(\omega)$, is given by the solid curve. (b) The individual contributions to the $N_2$–$O_2$ mixture part of $R(\omega, 300\ \mathrm{K})$ from the $N_2$ active quadrupolar and $O_2$ active hexadecapolar mechanisms, calculated within the isotropic polarizability approximation, are given by the dashed and dotted curves, respectively. The exact mixture contribution is given by the dash dotted curve.

The ratio of $\alpha_{\mathrm{air}}(\omega)$ to $\alpha_{\mathrm{N_2-N_2}}(\omega)$, $R(\omega, T)$, is plotted in Fig. 6 as a function of wavenumber $\omega(\mathrm{cm}^{-1})$ for four different temperatures. As can be seen from this figure, the ratio is relatively constant out to approximately $120\ \mathrm{cm}^{-1}$; it then increases with frequency and this increase is greater at lower $T$. The constant value $R(\omega, T) \approx 1.34$ is very close to the value (1.29) inferred by Pardo et al. [18] necessary to give improved agreement with their atmospheric observations. One can understand qualitatively this agreement for the low-frequency constant value by assuming that the "normalized" profiles for $O_2$–$O_2$, $N_2$–$N_2$, and $N_2$–$O_2$ are not very different. Thus the ratios

$$\alpha(\mathrm{O_2–O_2})/\alpha(\mathrm{N_2–N_2}) \approx S(\mathrm{O_2–O_2})/S(\mathrm{N_2–N_2})$$

Table 2
Comparison between the ratio of integrated intensities within the isotropic polarizability approximation; for mixtures, the first molecule in the parentheses is active and makes the rotational transition

| Ratio | Assumed by Pardo et al. [18] | Calculated here |
|---|---|---|
| $S(N_2–O_2)$ / $S(N_2–N_2)$ | 0.85 | 1.143 |
| $S(O_2–N_2)$ / $S(N_2–N_2)$ | 0.185 | 0.106 |
| $S(O_2–O_2)$ / $S(N_2–N_2)$ | 0.185 | 0.129 |

and

$$\alpha(N_2–O_2)/\alpha(N_2–N_2) \approx S(N_2–O_2)/S(N_2–N_2),$$

where the $S$'s are the integrated intensities. In this case using Eq. (9), the function $R(\omega, T)$ can be approximated by

$$R(\omega, T) \approx 1 + (0.0707)(0.129) + (0.266)(1.249) \approx 1.34, \tag{11}$$

where the first term from $O_2$–$O_2$ absorption is very small. In order to understand the increase with $\omega$, we can consider the isotropic polarizability approximation discussed above for the various absorptions. Assuming that the first molecule is the active one, that is the one that makes the rotational transition, we can compare the strength ratios used by Pardo et al. with the ones calculated in the present paper. This comparison is presented in Table 2.

In Fig. 7(a), we plot the three contributions to the function $R(\omega, 300\ \mathrm{K})$: $\alpha(N_2–N_2)/\alpha(N_2–N_2)(=1)$, $\alpha(N_2–O_2)/\alpha(N_2–N_2)$, and $\alpha(O_2–O_2)/\alpha(N_2–N_2)$, along with their sum. One can see that the absorption for the mixture increases with increasing wavenumber, reflecting both the double rotational transitions arising from the anisotropic induction mechanisms as well as the hexadecapole transitions having different selection rules. In Fig. 7(b), we plot the individual contributions to the $N_2$–$O_2$ mixture part of $R(\omega, 300\ \mathrm{K})$, calculated within the isotropic polarizability approximation, for the $N_2$ active quadrupolar and $O_2$ active hexadecapolar mechanisms, together with the "exact" theoretical curve. As can be seen, most of the increase with increasing wavenumber arises from the hexadecapolar transitions in $O_2$, which is consistent with the broader spectrum of $O_2$–$O_2$ in comparison with that of $N_2$–$N_2$.

## 5. Discussion and conclusions

In the present paper, we have analyzed the collision-induced translation-rotation spectra for $N_2$–$N_2$ and $O_2$–$O_2$ and showed that one can get good agreement between theory and experiment by increasing slightly the isotropic polarizability matrix element for $N_2$ and increasing the hexadecapole matrix element for $O_2$ by a factor 1.7 over the values found previously in a global analysis of the fundamental region. These changes will not affect the previous analyses of the fundamental spectra appreciably. Using the parameters obtained allows us to calculate theoretically the corresponding

absorption spectra for $N_2$–$O_2$ mixtures at different temperatures, and thus we can calculate the corresponding absorption coefficient for air. By factoring out the absorption for $N_2$–$N_2$, which is known accurately from previous theoretical calculations [22], we can obtain theoretically a correction function, $R(\omega, T)$, which can easily be incorporated into atmospheric models in order to go from pure $N_2$–$N_2$ to air.

By comparing our present results with those inferred by Pardo et al. [18], we can draw several conclusions: For wavenumbers up to 120 $cm^{-1}$, the correction factor is approximately constant and has the value of 1.34, very close to the value 1.29 inferred by Pardo et al. [18]. Above 120 $cm^{-1}$, it increases with wavenumber and this increase has a negative temperature dependence. We have showed that this increase is primarily due to the isotropic hexadecapole transitions in $O_2$ in the $N_2$–$O_2$ mixture contribution. The contribution in air due to the $O_2$–$O_2$ absorption is quite small vis-à-vis the other two contributions, reflecting the smallness of the quadrupole moment matrix element of $O_2$ compared to that of $N_2$.

The above results, together with the self ($H_2O$–$H_2O$) [25] and foreign ($H_2O$–$N_2$) [26] water continua, and the allowed lines given in the HITRAN database [27] permit one to model the continuous atmospheric absorptions very accurately in the far IR spectral region.

## Acknowledgements

Three of the authors (RHT, AB and QM) would like to acknowledge support from NASA through Grant No. NAG5-8269.

## References

[1] Ma Q, Tipping RH. The frequency detuning correction and the asymmetry of line shapes: the far wings of $H_2O$–$H_2O$. J Chem Phys 2002;116:4102–15.
[2] Ma Q, Tipping RH. The density matrix of $H_2O$–$N_2$ in the coordinate representation: a Monte Carlo calculation of the far-wing line shape. J Chem Phys 2000;112:574–84.
[3] Frommhold L. Collision-induced absorption in gases. Cambridge: Cambridge University Press, 1993.
[4] Edwards DP. GENLN2, Technical Note. NCAR, January 1992.
[5] Clough SA, Iacono MJ, Moncet JL. Line-by-line calculation of atmospheric fluxes and cooling rates: application to water vapor. J Geophys Res 1992;97:15,761–85.
[6] Boissoles J, Tipping RH, Boulet C. Theoretical study of the collision-induced fundamental absorption spectra of $N_2$–$N_2$ pairs for temperatures between 77 and 297 K. JQSRT 1994;51:615–27.
[7] Moreau G, Boissoles J, Boulet C, Tipping RH, Ma Q. Theoretical study of the collision-induced fundamental absorption spectra of $O_2$–$O_2$ pairs for temperatures between 193 and 273 K. JQSRT 2000;64:87–107.
[8] Moreau G, Boissoles J, Le Doucen R, Boulet C, Tipping RH, Ma Q. Experimental and theoretical study of the collision-induced fundamental absorption spectra of $N_2$–$O_2$ and $O_2$–$N_2$ pairs. JQSRT 2001;69:245–56.
[9] Moreau G, Boissoles J, Le Doucen R, Boulet C, Tipping RH, Ma Q. Metastable dimer contribution to the collision-induced fundamental absorption spectra of $N_2$ and $O_2$ pairs. JQSRT 2001;70:99–113.
[10] Long CA, Henderson G, Ewing GE. The infrared spectrum of $(N_2)_2$ van der Waals molecule. Chem Phys 1973;2:485–9.
[11] McKellar ARW. Infrared spectra of the $(N_2)_2$ and $N_2$-Ar van der Waals molecules. J Chem Phys 1988;88:4190–6.
[12] Maté B, Lugez CL, Solodov AM, Fraser GT, Lafferty WJ. Investigation of the collision-induced absorption by $O_2$ near 6.4 μm in pure $O_2$ and $O_2/N_2$ mixtures. J Geophys Res 2000;105:22,225–30.
[13] Stone NWB, Read LAA, Anderson A, Dagg IR, Smith W. Can J Phys 1984;62:338–47.

[14] Wishnow EH, Gush HP, Ozier I. Far-infrared spectrum of $N_2$ and $N_2$-noble gas mixtures near 80 K. J Chem Phys 1996;104:3511–6.
[15] Poll JD, Hunt JH. Analysis of the far infrared spectrum of gaseous $N_2$. Can J Phys 1981;59:1448–58.
[16] Birnbaum G, Cohen ER. Theory of line shape in pressure-induced absorption. Can J Phys 1976;54:593–602; Cohen ER, Birnbaum G. Influence of the potential function on the determination of multipole moments from pressure-induced far-infrared spectra. J Chem Phys 1977;66:2443–7.
[17] Bosomworth DR, Gush HP. Can J Phys 1965;42:751–7.
[18] Pardo JR, Serabyn E, Cernicharo J. Submillimeter atmospheric transmission measurements on Mauna Kea during extremely dry El Niño conditions: implication for broadband opacity contributions. JQSRT 2001;68:419–33.
[19] Steele WA, Birnbaum G. Molecular calculations of moments of the induced spectra for $N_2$, $O_2$, and $CO_2$. J Chem Phys 1980;72:2250–9.
[20] Poll JD, Hunt JH. On the moments of the pressure-induced spectra of gases. Can J Phys 1976;54:461–70.
[21] Ma Q, Tipping RH, Hartmann J-M, Boulet C. Detailed balance in far-wing line shape theories: comparisons between different formalisms. J Chem Phys 1995;102:3009–10.
[22] Borysow A, Frommhold L. Collision-induced rototranslational absorption of $N_2$–$N_2$ pairs for temperatures from 50 to 300 K. Astrophys J 1986;311:1043–57. A Fortran program to calculate this absorption can be obtained at: http://www.astro.ku.dk/~aborysow/programs/n2n2.good.for. The data for the correction factors plotted in Fig. 6 at 2.5 $cm^{-1}$ intervals can be obtained at: http://userwww.service.emory.edu/~abrown8/research/research.html.
[23] Zeiss GD, Meath WJ. Dispersion energy constants $C_6(A,B)$, dipole oscillator strength sums and refractivities for lithium, nitrogen atoms, oxygen atoms, hydrogen, nitrogen, oxygen, ammonia, water, nitric oxide, and nitrous oxide. Mol Phys 1977;33:1155–76.
[24] Orcutt RH, Cole RH. Dielectric constants of simplest gases. III. Atomic gases, hydrogen, and nitrogen. J Chem Phys 1967;46:697–702.
[25] Ma Q, Tipping RH. Water vapor continuum in the millimeter spectral region. J Chem Phys 1990;93:6127–39.
[26] Ma Q, Tipping RH. Water vapor millimeter wave foreign continuum: a Lanczos calculation in the coordinate representation. J Chem Phys 2002;117:10581–96.
[27] Rothman LS, Rinsland CP, Goldman A, Massie ST, Edwards DP, Flaud J-M, Perrin A, Camy-Peyret C, Dana V, Mandin JY, Schroeder J, McCann A, Gamache RR, Wattson RB, Yoshino K, Chance KV, Jucks JW, Brown LR, Nemtchinov V, Varanasi P. The HITRAN molecular spectroscopic database and HAWKS (HITRAN Atmospheric Workstation): 1996 edition. JQSRT 1998;60:665–710.